Published paper

Corkhill, CL, Bridge, JW, Chen, XC, Hillel, P, Thornton, SF, Romero-Gonzalez, ME, Banwart, SA and Hyatt, NC (2013) Real-Time Gamma Imaging of Technetium Transport through Natural and Engineered Porous Materials for Radioactive Waste Disposal. ENVIRONMENTAL SCIENCE & TECHNOLOGY, 47 (23). 13857 - 13864. Doi: 10.1021/es402718j

ACS AuthorChoice

Environmental Science & Technology

Article

pubs.acs.org/est

Real-Time Gamma Imaging of Technetium Transport through Natural and Engineered Porous Materials for Radioactive Waste Disposal

Claire L. Corkhill,*[,†,‡] Jonathan W. Bridge,[‡,§] Xiaohui C. Chen,[‡] Phil Hillel,[⊥] Steve F. Thornton,[‡] Maria E. Romero-Gonzalez,[‡] Steven A. Banwart,[‡] and Neil C. Hyatt[†]

[†]Immobilisation Science Laboratory, Department of Materials Science and Engineering, The University of Sheffield, Sheffield, South Yorkshire S1 3JD, United Kingdom

[‡]Kroto Research Institute, Department of Civil and Structural Engineering, The University of Sheffield, Sheffield, South Yorkshire S3 7HQ, United Kingdom

[§]Centre for Engineering Sustainability, School of Engineering, University of Liverpool, Liverpool, Merseyside L69 7ZX, United Kingdom

[⊥]Department of Nuclear Medicine, Sheffield Teaching Hospitals NHS Foundation Trust, Sheffield, South Yorkshire S10 2JF, United Kingdom

ABSTRACT: We present a novel methodology for determining the transport of technetium-99m, a γ-emitting metastable isomer of ^{99}Tc, through quartz sand and porous media relevant to the disposal of nuclear waste in a geological disposal facility (GDF). Quartz sand is utilized as a model medium, and the applicability of the methodology to determine radionuclide transport in engineered backfill cement is explored using the UK GDF candidate backfill cement, Nirex Reference Vault Backfill (NRVB), in a model system. Two-dimensional distributions in ^{99m}Tc activity were collected at millimeter-resolution using decay-corrected gamma camera images. Pulse-inputs of ~20 MBq ^{99m}Tc were introduced into short (<10 cm) water-saturated columns at a constant flow of 0.33 mL min^{-1}. Changes in calibrated mass distribution of ^{99m}Tc at 30 s intervals, over a period of several hours, were quantified by spatial moments analysis. Transport parameters were fitted to the experimental data using a one-dimensional convection−dispersion equation, yielding transport properties for this radionuclide in a model GDF environment. These data demonstrate that ^{99}Tc in the pertechnetate form ($Tc(VII)O_4^-$) does not sorb to cement backfill during transport under model conditions, resulting in closely conservative transport behavior. This methodology represents a quantitative development of radiotracer imaging and offers the opportunity to conveniently and rapidly characterize transport of gamma-emitting isotopes in opaque media, relevant to the geological disposal of nuclear waste and potentially to a wide variety of other subsurface environments.

INTRODUCTION

The waste arising from >60 years of civil and military nuclear operations around the world contains long-lived radionuclides that must be contained and isolated from future populations. Deep geological disposal facilities (GDF) proposed by US and European waste management organisations[1−4] employ an engineered multibarrier approach (Figure 1) to retard the release of radioactive species from the waste in quantities that could be detrimental to life and the environment. The multibarrier design concept typically combines reducing conditions with high pH with the purpose of limiting the solubility and mobility of radionuclide species within GDF if (or when) primary containment fails.[4]

A significant obstacle to implementation of GDF is public and political concern around risks and consequences of failure against design criteria over the 10^5 to 10^6 year required lifespan of the facility,[4] highlighted by several failures to site GDF repositories, e.g., in the UK[5,6] and at Yucca Mountain in the USA.[7] Should GDF performance be compromised, it is possible that long-lived, mobile radionuclides will be transported through the engineered backfill into groundwater and pose a long-term hazard to the biosphere and water resources. Thus, it is critical to the safety case for the GDF not only to be able to demonstrate that the design performance is well understood but to show that conditions arising from design failures are also accounted for and mitigated as far as possible.

One potentially problematic radionuclide is technetium-99, a high-yield fission product of ^{235}U, which has a long half-life (2.1×10^5 years) and high solubility in oxic conditions as the pertechnetate anion [$Tc(VII)O_4^-$]. While the conditions within the GDF are expected to be reducing, such that insoluble Tc(IV) should be the dominant oxidation state, the UK nuclear authority estimates suggest that a significant proportion of the

Received: June 19, 2013
Revised: October 15, 2013
Accepted: October 22, 2013
Published: October 22, 2013

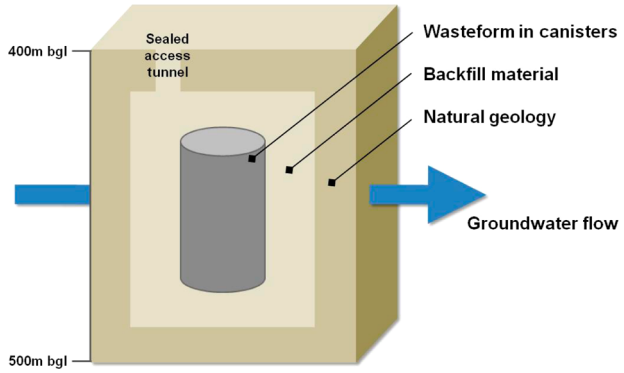

Figure 1. General design features of the multibarrier geological disposal facility (GDF) concept proposed for the long-term (~10^6 year) storage of high-level nuclear wastes in the deep subsurface (bgl = below ground level). Material design should be optimized to resist groundwater ingress and contaminant migration.

UK ^{99}Tc inventory is expected to be present as the Tc(VII) pertechnetate species.[8] Performance assessment analysis of Tc mobility has shown that the potential risk to future populations from ^{99}Tc critically depends upon its oxidation state,[8] such that Tc(VII) presents a significantly greater risk than Tc(IV) over the one million year lifetime of the GDF, even when reducing conditions are applied. Therefore, a robust design for the engineered barrier concept should be able to account for the risk arising from the presence and behavior of the mobile Tc(VII), separately from the specific probability of oxic conditions occurring or persisting within any given GDF scenario. An improved understanding of the behavior of pertechnetate in proposed barrier materials is also necessary to evaluate the potential of different design specifications to mitigate or remove the potential hazard.

Understanding the spatial and temporal dynamics of geochemistry within and surrounding a GDF is essential in this task. The importance of (bio)geochemical gradients on radionuclide mobility is the focus of substantial current research, e.g., refs 9−11. Such studies ideally require noninvasive, nondestructive measurement of the distribution, migration, and chemical transformation of radionuclides within a physical model of the barrier material. This should be considered over time as internal conditions respond to controlled changes in boundary conditions.

Quantitative imaging techniques offer a means of achieving this information and have been developed to study reactive transport in porous media for a range of materials. Imaging techniques include visible light transmission and fluorescence imaging,[12,13] nuclear magnetic resonance (NMR), and X-ray computed tomography (see ref 14 for a recent review). Gamma attenuation techniques with external americium-241 or cesium-137 sources have been used to determine fluid transported within a column.[15] A key methodological step remains: the extraction of quantitative geochemical information from image data, particularly in three dimensions and opaque materials.[14] Techniques have been developed to quantify, from image data, pH and oxygen gradients in two dimensions (2D) within porous media[16] and to extract transport, deposition, and remobilization rate parameters from time-lapse image sequences of colloidal particles in translucent quartz sand.[13,17] Recent work demonstrated that gamma-emitting radioisotopes can be used as an effective imaging tracer within opaque sediment and mineral systems, both in static batch experiments[18,19] and in flow-through columns.[20] These studies utilized ultratrace concentrations of a gamma-emitting technetium isotope, technetium-99m (commonly used in medical and industrial imaging applications), to demonstrate qualitatively the immobilization of technetium on Fe(II)-bearing sediments and minerals, via an Fe(II)-mediated reduction of Tc(VII) to Tc(IV).

In this study, we report the use of 2D gamma-imaging to quantify ^{99m}Tc transport parameters in a simple granular porous media model. Uniform, saturated one-dimensional flow through Ottawa quartz sand, as a model test material, is used to demonstrate the ability of gamma imaging to obtain reproducible data sets at the mesoscale (millimeters to decimeters), which can be used to yield transport parameters by fitting standard convection−dispersion models. Furthermore, we apply this methodology, for the first time, to investigate the feasibility of direct noninvasive quantification of radionuclide migration within opaque cementitious GDF candidate material (crushed Nirex Reference Vault Backfill (NRVB)[21]) under circum-neutral and alkaline pH. The technique represents a base for development of model systems for noninvasive study of radionuclide migration in complex physicochemical environments, critical to establishing the design specifications and safety case for future GDFs, and also for application to other contaminant transport in the subsurface.

EXPERIMENTAL SECTION

Replicated flow cells enabled aqueous solutions with and without a ^{99m}Tc tracer to be pumped through saturated quartz sand at a steady flow rate with continuous monitoring using a gamma camera. ^{99m}Tc is a controlled radioactive substance; therefore, experiments were performed with appropriate risk assessment in specialist facilities at a hospital which routinely produces and handles the material for use in clinical nuclear medicine. All other chemicals used were obtained from Fisher Scientific (UK) unless otherwise indicated.

Flow Cell Design and Setup. Bench-scale flow cells were constructed of two Perspex plates separated by Viton seals and bolted tightly together (Figure 2). The rear plate was solid,

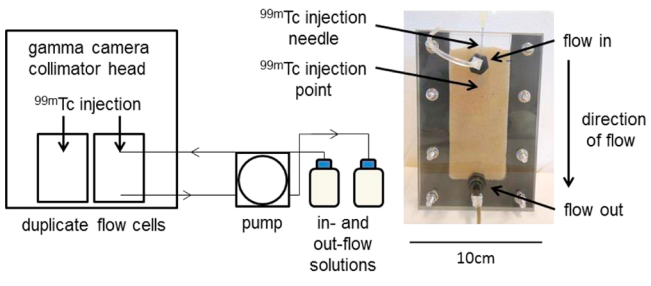

Figure 2. Schematic of the experimental setup showing construction of the flow cells, the pumping system, and image acquisition geometry.

while the front plate had an indent creating a void space to hold the porous material. When assembled, the internal void was 100 × 50 × 7 mm. An upper port in the rear plate allowed for input of the aqueous phase to the cell, while a lower port in the same plate allowed for removal of the aqueous phase for control of flow rate and sampling. Flow was from top to bottom along a distance of 70 mm between the ports. ^{99m}Tc tracer was injected through a needle immediately below the inlet port (Figure 2).

The flow cells were filled with 70 g of Ottawa sand (99.5% SiO_2, particle diameter 500−700 μm) or 45 g of crushed Nirex Reference Vault Backfill (NRVB),[21] sieved to 2−4 mm particle size, ensuring maintenance of appropriate flow rates. Crushing and experimental setup were conducted in air several hours prior to experimentation, in which time some carbonation of the exposed surfaces may have taken place. The possible chemical changes that might be expected for degraded backfill are outside the scope of the current study and are thus not addressed in this model GDF system. The sand was washed and sonicated in ultrahigh quality water (18 MΩ) five times to remove any existing impurities and oven-dried for 24 h prior to use. The NRVB material was prepared by mixing 130.1 g of Ordinary Portland Cement, 49.12 g of $Ca(OH)_2$, 143.1 g of $CaCO_3$, and 177.76 mL of water in a Hobart mixer, giving a w/s ratio of 0.552. It was cured at room temperature for 28 days and kept sealed prior to use. Duplicate flow cells containing sand were saturated with 16 mL of pH 5.7, deionized water (18 MΩ) so that the material plus aqueous phase filled the cell above the inlet port. A 3 mm depth of solution was maintained above the top of the material to ensure a uniform pressure head across the flow field. Identical flow cells were prepared using a pH 10.7 buffer solution (0.05 M $NaHCO_3$, 0.1 M NaOH). A flow cell containing NRVB was saturated with 25 mL of deionized water at pH 5.7 (18 MΩ). The pH within these flow cells quickly equilibrated to pH ∼12. The porosity calculated from the ratio of solution volume to total saturated pack volume was 0.37 for sand and approximately 0.77 for the crushed NRVB, taking into account the internal porosity of the material itself (estimated as 0.55[21]). Bulk densities of the porous materials as packed were 1.68 and 1.57 kg dm^{-3} for sand and NRVB, respectively.

Gamma Camera Imaging of Technetium-99m in Steady Saturated Flow. Fully constructed, prefilled flow cells were transported to the Nuclear Medicine Department of the Royal Hallamshire Hospital (Sheffield, UK) for imaging. Duplicate flow cells were placed <3 cm from the collimator face. Flow was maintained in the cells at 0.33 mL min^{-1} using a multichannel peristaltic pump (Watson Marlow, UK), yielding a calculated pore velocity equal to 4.29×10^{-5} m s^{-1} for the sand and 2.05×10^{-5} m s^{-1} for the NRVB (due to the greater porosity). The Darcy flux in both cases was 1.5×10^{-5} m s^{-1}. Flow cells were flushed with ^{99m}Tc-free solution for 20 min to establish uniform flow conditions prior to injection with ^{99m}Tc and subsequent imaging. Imaging was performed on a dual-headed GE Medical Systems Infinia gamma camera (GE Medical, Milwaukee, WI, USA) fitted with a high resolution collimator. A dynamic acquisition with 30 s frame intervals was initiated a few seconds prior to injection of the ^{99m}Tc into the flow cells. Images were acquired with a matrix size of 256 × 256 resulting in a pixel size of 2.2 mm. The spatial resolution of the imaging system was measured at the collimator face using standard NEMA[22] testing techniques and was found to be 4.6 mm FWHM. This equates to a spatial resolution of ∼6 mm at the location of the flow cells. Due to the low spatial resolution, measurements were made at the center of the ^{99m}Tc tracer plume.

^{99m}Tc Tracer. ^{99m}Tc as pertechnetate [Tc(VII)] was produced on-site via saline-based elution of a GE Medical Systems Drytec ^{99m}Tc generator. Approximately 0.2 mL of dilute ^{99m}Tc was drawn into a syringe. This volume gave an activity of 15−20 MBq at the time of the experiment. This corresponds to ^{99m}Tc concentrations of <1 mM. The activity in each syringe was accurately measured in a Capintec CRC-15R radionuclide calibrator. Following injection of the ^{99m}Tc into the flow cells as instantaneous pulses (<1 s injection), the residual activity in each syringe was measured and this reading was subtracted from the "full" reading to determine the exact activity injected into each cell. In all cases, ^{99m}Tc activity readings were decay-corrected to the time the gamma camera acquisition was started (eq 1, 2):

$$A_0 = A_t e^{kt} \tag{1}$$

$$k = \frac{\ln 2}{t_{1/2}} \tag{2}$$

where A_0 is the corrected activity (MBq), A_t is the uncorrected activity (MBq), k is the decay constant (s^{-1}), t is the time elapsed (s), and $t_{1/2}$ is the half-life of ^{99m}Tc (21 636 s). For each flow cell, a sensitivity value (counts per MBq) was determined so that image counts could be related directly to ^{99m}Tc activity. This sensitivity value was calculated by using region of interest (ROI) analysis to determine the image counts per frame within the region of the cell, averaged over the first 4 frames following injection of the radioisotope. During this early period, all the activity remained in the cell near the inlet. This averaged count value was then divided by the known activity injected into the cell to yield a sensitivity factor (eq 3):

$$\mathrm{Sf} = \frac{\overline{x}_{ci}}{A_0} \tag{3}$$

where Sf is the sensitivity factor, $\overline{x}_{ci}$ is the mean of the counts from the first four frames of image acquisition (counts $pixel^{-1}$), and A_0 is the initial activity (MBq). This sensitivity factor was applied to all decay-corrected gamma counts throughout the experiments to yield the concentration C (MBq $pixel^{-1}$, normalized by the volume of pores in each pixel to give MBq mL^{-1}) of ^{99m}Tc at any location in each time step.

Data Processing and Analysis. Raw image data were calibrated using the sensitivity factor (eq 3) to give 2-D planar spatial arrays of tracer concentration data at 30 s intervals for up to 3 h during and after transit of the main mass of ^{99m}Tc through the flow cell. Spatial moments in the direction of travel were calculated at the center of mass of the plume using ImageJ software.[23] Calibrated concentration maps showing contours of ^{99m}Tc mass within the flow cells were produced by interpolation of the 2-D data arrays using Surfer 9.0 software (Golden software, CA). The transport of the ^{99m}Tc through the uniform saturated flow field was modeled using a one-dimensional (1-D) convection−dispersion equation for reactive solute transport (eq 4):

$$R\frac{\partial C}{\partial t} = D\frac{\partial^2 C}{\partial x^2} - V_p\frac{\partial C}{\partial x} - \mu C \tag{4}$$

where, subject to specified initial and boundary conditions, C is the aqueous concentration of a tracer at a given distance along the center of mass from inlet x (m) and elapsed time t (s), μ (s^{-1}) is a first-order decay coefficient describing irreversible removal from the mobile aqueous phase, R is a retardation factor describing equilibrium interaction with the solid phase, and D is a dispersion coefficient equal to the product of the longitudinal dispersivity λ (m) and mean pore flow velocity, V_p (m s^{-1}). A numerical solution to eq 4 was implemented in inverse (parameter-fitting) mode in Excel-CXTFIT software[24]

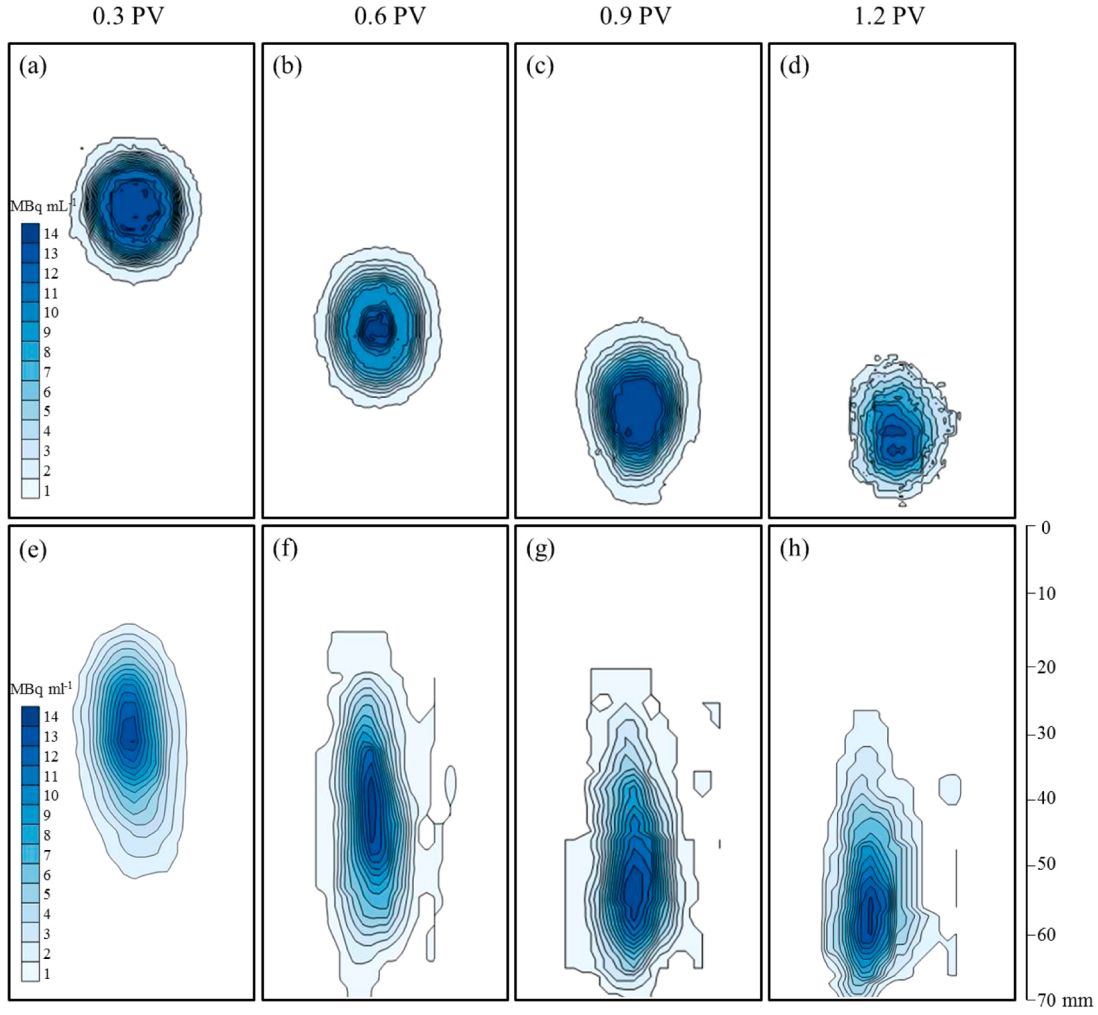

Figure 3. Calibrated concentration distribution from gamma camera images of ^{99m}Tc activity in Ottawa quartz sand in a pH 5.7 solution at (a) 0.29 PV (8 min), (b) 0.58 PV (16 min), (c) 0.87 PV (24 min), and (d) 1.16 PV (32 min) and in Nirex Reference Vault Backfill at (e) 0.3 PV (20 min), (f) 0.6PV (40 min), (g) 0.9 PV (60 min), and (h) 1.2 PV (80 min).

to yield transferable parameters describing the transport of the radionuclide in the Ottawa quartz sand and NRVB.

RESULTS AND DISCUSSION

^{99m}Tc Transport within Ottawa Quartz Sand. Figure 3a–d shows the calibrated concentration distribution data for ^{99m}Tc transport through the Ottawa sand at pH 5.7, at 8 (0.29), 16 (0.58), 24 (0.87), and 32 (1.16) minutes after injection. Values in parentheses and all time data thereafter are expressed in pore volumes (PV), where time is normalized by the transit time of a volume of solution equal to the volume of void spaces in the sand. Under the conditions of these experiments, 1 PV was equivalent to 1650 s (27.5 min) of travel time. The ^{99m}Tc tracer passed through the saturated sand as well-defined plumes with peak concentrations in the center approximately 10 ± 2 MBq mL^{-1}. Figure 4 shows the total ^{99m}Tc activity measured in the sand as a function of time for experiments at pH 5.7 and 10.7. Total activity decreased rapidly around 1 PV, as expected for conservative transport. This behavior was highly reproducible for experimental runs at both pH 5.7 and 10.7. Residual activities measured after 2 PV (not shown) were less than 1% of the total activity injected and were not significantly different from zero, taking into account the assumed measurement error

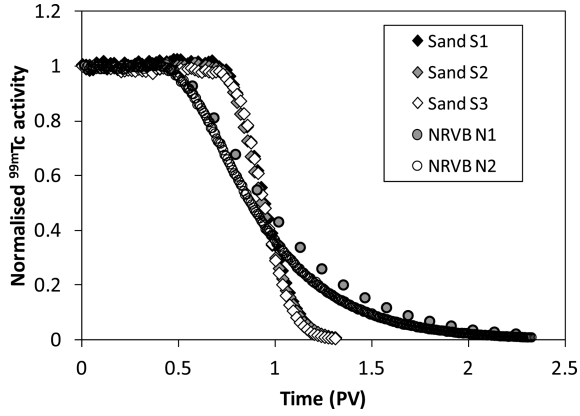

Figure 4. Total measured activity of ^{99m}Tc (normalized to input activity) as a function of time (expressed as PV, normalized to flow rate) during transport through Ottawa quartz sand S1 and S2 at pH 5.7 and S3 at pH 10.7 and NRVB.

quantified by the standard deviation (±1%) for total activity measurements made between 0.25 and 0.5 PV.

^{99m}Tc Transport within NRVB. Figure 3e–h shows calibrated concentration distributions for ^{99m}Tc transport in NRVB at 0.3, 0.6, 0.9, and 1.2 PV. Due to the lower pore

dx.doi.org/10.1021/es402718j | Environ. Sci. Technol. 2013, 47, 13857–13864

Table 1. Modelled Transport Parameters for ^{99m}Tc under Uniform Flow through Saturated Quartz Sand and NRVB

		solution pH						sorption coefficient, K_d, $\times 10^{-5}$ (m^3 kg^{-1})		
media	run	start	end	injected activity (MBq)	velocity $\times 10^{-5}$ (m s^{-1})	dispersivity, λ, $\times 10^{-5}$ (m)	retardation, R	M1	M2	M3
sand	S1	5.7	5.8	15.02	4.24 ± 0.43	0.96 ± 0.07	1.00 ± 0.01	1.19	0.29 ± 0.08	0.13
	S2	5.7	5.8	11.29	4.23 ± 0.43	1.05 ± 0.08	1.02 ± 0.01			
	S3	10.7	10.7	16.62	4.24 ± 0.17	0.90 ± 0.01	1.02 ± 0.00			
NRVB	N1	12	12	13.32	1.64 ± 0.50	3.30 ± 1.10	1.08 ± 0.38	1.27	6.90 ± 25.50	4.85
	N2	12	12	24.80	1.65 ± 0.43	3.49 ± 0.85	1.05 ± 0.28			

velocities in NRVB than in sand, 1 PV was equivalent to 4300 s (71.5 min) of travel time. ^{99m}Tc was transported through the NRVB in an elongate but still coherent plume. The peak concentration at 0.3 PV was 12 MBq mL^{-1}, measured at ~3 cm from the injection point. After 0.6, 0.9, and 1.2 PV, the peak concentrations were measured as 10, 9, and 8 MBq mL^{-1}, respectively, at ~4, 5.5, and 6 cm from the tracer injection point (Figure 3).

The total ^{99m}Tc activity measured in the NRVB as a function of time is shown in Figure 4. As in sand, total activity decreased broadly symmetrically around 1 PV, indicating conservative transport with longitudinal dispersion. Residual activity at the end of the measurement period was less than 2% of the initial activity and not significantly different from zero, taking into account variability in the image data quantified as noted above.

Numerical Modeling of ^{99m}Tc Transport Parameters. ^{99m}Tc activity was summed across horizontal pixel rows (normal to the vertical direction of transport through the cells) to yield concentration profiles which could be expressed as a function of distance from inlet or time since tracer injection. These data were fitted with the 1-D convection−dispersion model (eq 4). In individual experiment runs S1−S3 and N1−N2 (Table 1), the model was regressed to concentration profiles measured at five distances from the inlet simultaneously, using the linear least squared error method.[24] The best fit model parameters for each experiment condition are shown in Table 1; irreversible sorption parameter μ was never larger than zero and is therefore not tabulated. Figure 5a compares data from an individual experiment run in sand with the output from the model run in forward mode for the same distance intervals, using averages of the parameter values shown in Table 1. The correlation between the model and data is very strong (r^2 = 0.98). Figure 5b shows equivalent data and model output (r^2 = 0.99) for NRVB.

The parameters obtained from numerical modeling of ^{99m}Tc transport in sand (Table 1) strongly indicate conservative transport (R = 1) of the ^{99m}Tc through the Ottawa quartz sand. This conclusion is supported by independent spatial moments analysis of the calibrated image data (Figure 6), which yields a mean velocity for the center of mass of the ^{99m}Tc plumes in sand of 4.32×10^{-5} m s^{-1}. The transport velocity for the ^{99m}Tc was therefore not significantly different from the pore velocity in the quartz sand (4.29×10^{-5} m s^{-1}) calculated a priori. In contrast, both spatial moments and numerical modeling yielded the same mean transport velocity for ^{99m}Tc transport through NRVB, 1.64×10^{-5} m s^{-1}, which was slower than the calculated pore velocity based on the internal and boundary conditions of the experiment (2.05×10^{-5} m s^{-1}). This may be due to errors in estimation of the internal pore structure of the NRVB which may be discontinuous, creating regions of low flow or immobile pore water. While R remained close to 1 indicating conservative

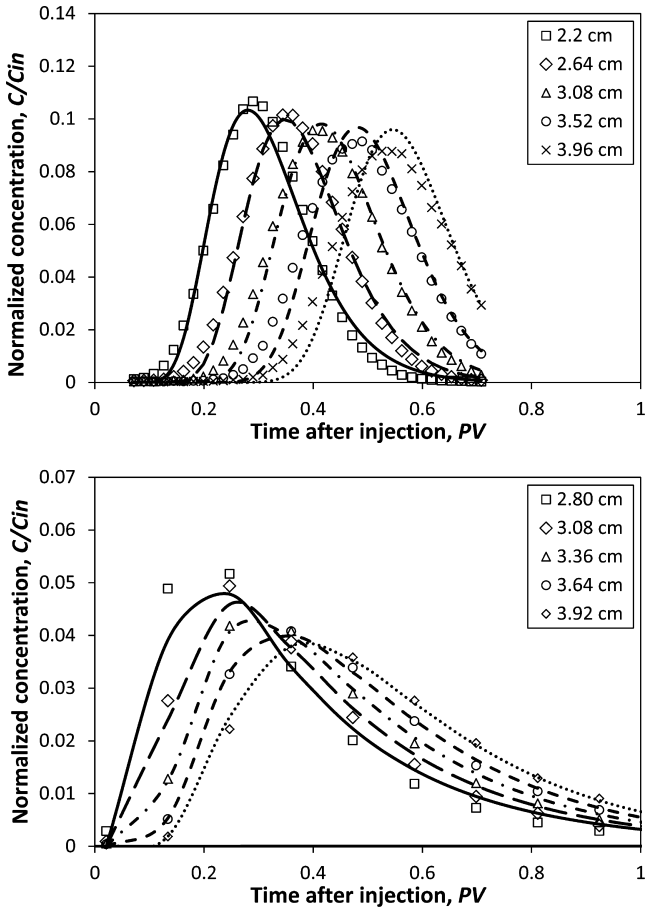

Figure 5. Best fit numerical regression of a convection−dispersion model (lines) to measured ^{99m}Tc concentrations (data points) in (a) Ottawa quartz sand and (b) NRVB material at several distances from the inlet during uniform saturated flow.

transport, the longitudinal dispersivity, λ, for NRVB was 0.0033 m, more than three times that modeled in sand.

Estimation of Sorption Coefficients from Tc Transport Data. The sorption of solutes to a solid phase is often described by an equilibrium linear sorption coefficient K_d (m^3 kg^{-1}) estimated from batch experiments, which contain a known volume of solution, concentration of solute, and mass of solid phase, yielding (eq 5):

$$K_d = \frac{C_s}{C_0}\frac{V}{m} \quad (5)$$

where C_0 and C_s are, respectively, the initial solute concentration in solution and final equivalent concentration on the solid phase, m (kg) is the mass of solid phase, and V (m^3) is the volume of the fluid. We approximated these parameters by normalizing the known input activity and the

dx.doi.org/10.1021/es402718j | Environ. Sci. Technol. 2013, 47, 13857−13864

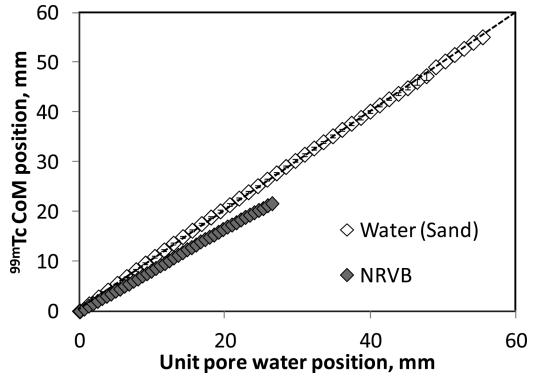

Figure 6. Tracer plume center of mass (CoM, first spatial moment in the direction of flow) plotted as a function of calculated water movement for ^{99m}Tc transport through Ottawa quartz sand and NRVB. Dashed line indicates direct $y = x$ correlation. Data are averages of experimental replicates.

observed retained activity by the volume and mass of porous media in the flow chamber, to obtain an estimate for K_d (we denote this method M1). For reactive transport through porous media and assuming that surface reactions occur sufficiently rapidly relative to transport that equilibrium can be achieved, K_d can also be related both to the retardation factor R in the convection−dispersion equation (denoted method M2) and to the ratio of mean transport velocities obtained from spatial moments analysis (method M3) by eq 6:[25]

$$R = 1 + \frac{\rho_b K_d}{\varepsilon} = \frac{V_p}{V_{Tc}} \quad (6)$$

where ε is the porosity, ρ_b is the bulk density (kg m^{-3}) of the porous media, and V_{Tc} is the mean velocity of mass flux (m s^{-1}). We estimated K_d by all three methods M1−M3 (Table 1).

Estimated sorption coefficients for both sand and NRVB were small, of the order 10^{-5} m^3 kg^{-1}, which is consistent with the transport parameters obtained from the convection−dispersion modeling and the observed low retention of ^{99m}Tc in the sand after 2 PV. Although the model-derived errors associated with NRVB were relatively large, K_d as estimated by all three methods was consistently greater in NRVB (approximately an order of magnitude) than in sand (Table 1). We reiterate that K_d as calculated assumes equilibrium in the underlying sorption reactions; however, we cannot confirm this with the data reported here and, as such, our values may be biased toward underestimation. We do note, however, the empirical observation that after a relatively short period of flushing of the mobile ^{99m}Tc plume from the flow chamber, less than 1−2% remained suggesting that the sorption that does occur within the transit time of the plume may be readily and rapidly reversible when solute concentrations return to zero, for both materials under these experimental conditions. We are also aware of the possibility that some irreversible sorption (1−2%) may occur as it is hard to rule out this condition without sorption capacity measurements.

Applicability of Quantitative γ-Imaging Transport of Radionuclides and Other Contaminants in Opaque Media. In the interpretations that follow, we recognize that several assumptions and simplifications have been made in the model GDF systems investigated. These have been made in order to demonstrate the applicability of the gamma imaging technique to radionuclide transport in a GDF and, as such, provide the basis for future detailed experimentation.

The limited retardation ($R \approx 1$) interpreted using the model, very low estimated K_d obtained with the different methods, and the minimal retention of ^{99m}Tc in the sand at the end of the experiments imply closely conservative transport of ^{99m}Tc through Ottawa sand. Although this is the first time that this has been confirmed directly, it is not an unexpected result. The point of zero charge (PZC) of Ottawa sand is between pH 2 and 5,[26] so at the pH of these experiments (>5.7), the sand surface is negatively charged. Since the pertechnetate anion (TcO_4^-) is also negatively charged, chemical sorption is therefore impeded by repulsive electrostatic interactions between the Tc and sand. This indicates that Tc(VII) may be transported freely in environments where the substrate has only negatively charged surfaces. Such pure-phase interactions are a simplification of natural environments, especially where significant quantities of Fe(II) or other minerals capable of reducing Tc(VII) to the less mobile and less soluble Tc(IV) are present or in environments where microbially mediated reactions may take place to alter the oxidation state of technetium. Nevertheless, these results highlight the utility of quantitative measurements of transport parameters for Tc(VII) in opaque porous media, that may be applied to substrate related to GDF concepts (e.g., clay, host rock).

We have shown that it is possible to obtain quantitative transport data using the gamma imaging technique in opaque engineered backfill material. Pertechnetate transport in NRVB in our GDF-proxy experiments was closely conservative, i.e., our data pertaining to ^{99m}Tc transport in this material showed no significant retardation and very low sorption coefficients. Previous studies have suggested low sorption coefficients for Tc(VII) in batch experiments using aged, crushed NRVB,[27,28] and our study indicates, for the first time using quantitative imaging, that such observations may translate into a significant potential for transport of ^{99}Tc(VII) through a backfill candidate material in a model flowing groundwater system. Despite the low spatial resolution of the gamma images, ^{99m}Tc transported through NRVB exhibited a greater dispersivity and slower transport velocity than in sand. This is likely due to the very high internal porosity. Discontinuities in the internal structure may create significant immobile (very low flow) zones within the pore space. Further work on NRVB will explore the use of a mobile-immobile (MIM) transport model (e.g., Tang et al.[24]), to better elucidate the dynamics of solute transport through this material.

The quantitative gamma imaging technique described in this paper represents a rapid and convenient method for obtaining transport data for ^{99m}Tc. The main advantage of this technique is that quantitative images can be obtained in opaque media; it is possible to see the retained mass as a function of time and space, allowing for a direct visual quantification of transport parameters. Furthermore, in experiments where the sorption can be controlled for, it may be possible to visualize and quantify sorption. This multitude of information is such that transport models, such as CXTFIT used here to test and validate the methodology, may not be required to derive transport parameters. High spatial resolution is important to gain an accurate measurement of dispersivity. The spatial resolution presented in this methodology was relatively low (6 mm), largely as an artifact of the spatial constraints placed upon using a working hospital camera. However, higher spatial resolution, and thus accurate dispersivity measurements, should

be possible, depending upon the quality of the instrument and proximity to the collimator.

Quantitative gamma imaging has several potential applications to contaminant transport in opaque media. In the context of geological disposal of nuclear waste, the transport of ^{129}I from the waste and through the engineered barrier is a key concern due to its long half-life (15.7×10^6 years), high solubility, and poor sorption.[27−29] Gamma imaging coupled with the γ-emitting ^{123}I radiotracer could be used to develop an understanding of iodine transport behavior and thus support engineered barrier material design. Because the gamma camera can detect ultratrace concentrations of radionuclides, several gamma-emitting isotopes could also be used to nondestructively quantify the transport of environmental contaminants in soil, such as chromium (^{51}Cr) or mercury (^{203}Hg). This highlights the potential versatility of the technique, applicable to a wide range of scenarios as a novel tool to understand the spatial and temporal dynamics of the geochemistry of a variety of radiotracers in opaque media.

AUTHOR INFORMATION

Corresponding Author

*E-mail: c.corkhill@sheffield.ac.uk; tel: +44 (0)114 2226036.

Notes

The authors declare no competing financial interest.

ACKNOWLEDGMENTS

C.L.C. would like to acknowledge financial support from the EPSRC under Grant EP/F055412/1 (Decommissioning Immobilisation and Management of Nuclear wastes for Disposal) and The University of Sheffield for the award of a Vice Chancellor's Fellowship. We are grateful to Dr. Claire Utton for assistance with NRVB synthesis. N.C.H. is grateful to the Royal Academy of Engineering and the Nuclear Decommissioning Authority for funding. X.C.C. and S.F.T. gratefully acknowledge support from NERC under Grant NH/H006540/1: BIogeochemical Gradients and RADionuclide Transport. The authors are extremely grateful to an anonymous reviewer for their suggestions to improve the manuscript.

REFERENCES

(1) Zuloaga, P.; Astudillo, J. The Spanish Radioactive Waste Management and the associated research ensuring its development from sound technical to scientific basis. *Mater. Res. Soc. Symp. Proc.* **2012**, *1475*, 25−36.

(2) Andersson, J.; Skagius, K.; Winberg, A.; Lindborg, T.; Strom, A. Site-descriptive modelling for a final repository for spent nuclear fuel in Sweden. *Environ. Earth Sci.* **2013**, *69*, 1045−1060.

(3) Patel, P.; Ewing, R. United States launches new direction to manage nuclear waste. *MRS Bull.* **2013**, *38*, 206−207.

(4) *Geological Disposal, Steps toward implementation*, NDA/RWMD/013; Nuclear Decommissioning Authority: Oxon, UK, March 2010.

(5) *Managing Radioactive Waste Safely: A framework for Implementing Geological Disposal*, UK Government White Paper number Cm7836; Crown: Surrey, June 2008.

(6) *Managing Radioactive Waste Safely: Call for evidence on the siting process for a geological disposal facility*, UK Department of Energy and Climate Change Public Consultation document, URN 13D/105; Crown: Surrey, 13th May 2013.

(7) *Effects of termination of the Yucca Mountain Repository Programme and Lessons Learned*, United States Government Accountability Office, GAO-11-229; GAO: Washington, DC, April 2011.

(8) *Generic Repository Studies: Generic post-closure Performance Assessment*, Report number N/080; United Kingdom Nirex Limited: Oxfordshire, UK, 2003.

(9) Rizoulis, A.; Steele, H.; Morris, K.; Lloyd, J. The potential impact of anaerobic microbial metabolism during the geological disposal of intermediate-level waste. *Mineral. Mag.* **2012**, *76*, 3261−3270.

(10) Beattie, T. M.; Williams, S. J. An overview of near-field evolution research in support of the UK geological disposal programme. *Mineral. Mag.* **2012**, *76*, 2995−3001.

(11) Yang, Y.; Saiers, J. E.; Minasian, S. G.; Tyliszczak, T.; Kozimor, S. A.; Shuh, D. K.; Barnett, M. O. Impact of natural organic matter on uranium transport through saturated geologic materials: From molecular to column scale. *Environ. Sci. Technol.* **2012**, *11*, 5931−5938.

(12) Huang, W. E.; Smith, C. C.; Lerner, D. N.; Thornton, S. F.; Oram, A. Physical modelling of solute transport in porous media: Evaluation of an imaging technique using UV excited fluorescent dye. *Water Res.* **2002**, *36*, 1843−1853.

(13) Bridge, J. W.; Banwart, S. A.; Heathwaite, A. L. Non-invasive quantitative measurement of colloid transport in mesoscale porous media using time lapse fluorescence imaging. *Environ. Sci. Technol.* **2006**, *40*, 5930−5936.

(14) Werth, C. J.; Zhang, C.; Brusseau, M. L.; Oostrom, M.; Baumann, T. A review of non-invasive imaging methods and applications in contaminant hydrology research. *J. Contam. Hydrol.* **2010**, *113*, 1−24.

(15) Crestana, S.; Vaz, C. M. P. Non-invasive instrumentation opportunities for characterising soil I porous systems. *Soil Tillage Res.* **1998**, *47*, 19−26.

(16) Rudolph, N.; Esser, H. G.; Carminati, A.; Moradi, A. B.; Hilger, A.; Kardjilov, N.; Nagl, S.; et al. Dynamic oxygen mapping in the root zone by fluorescence dye imaging combined with neutron radiography. *J. Soils Sediments* **2011**, *12*, 63−74.

(17) Bridge, J. W.; Heathwaite, A. L.; Banwart, S. A. Measurement of colloid mobilisation and re-deposition during drainage in quartz sand. *Environ. Sci. Technol.* **2009**, *43*, 5769−5775.

(18) Burke, I. T; Livens, F. R.; Lloyd, J. R.; Brown, J. R.; Law, G. T. W.; McBeth, J. M.; Ellis, B. L.; Lawson, R. S.; Morris, K. The fate of technetium in reduced esturine sediments: Combining direct and indirect analyses. *Appl. Geochem.* **2010**, *25*, 233−241.

(19) Lear, G.; McBeth, J. M.; Boothman, C.; Gunning, D. J.; Ellis, B. L.; Lawson, R. S.; Morris, K.; Burke, I. T.; Bryan, N. D.; Brown, A. P.; Livens, F. R.; Lloyd, J. R. Probing the biogeochemical behaviour of technetium using a novel nuclear imaging approach. *Environ. Sci. Technol.* **2010**, *44*, 156−162.

(20) Cutting, R. S.; Coker, V. S.; Telling, N. D.; Kimber, R. L.; Pearce, C. I.; Ellis, B. L.; Lawson, R. S.; Van Der Laan, G.; Pattrick, R. A. D.; Vaughan, D. J.; Arenholz, E.; Lloyd, J. R. Optimising Cr(VI) and Tc(VII) remediation through nanoscale biomineral engineering. *Environ. Sci. Technol.* **2010**, *44*, 2577−2584.

(21) *Development of the Nirex Reference Vault Backfill*; Report on current status in 1994, Report number S/97/014; United Kingdom Nirex Limited: Oxfordshire, UK, 1997.

(22) *Performance measurements of gamma cameras*. NU 1-2012, NEMA Standards Publication; NEMA: Rosslyn, Virginia, 2013.

(23) Rasband, W. S. *ImageJ*; U. S. National Institutes of Health: Bethesda, Maryland, USA, 1997−2012; http://imagej.nih.gov/ij/.

(24) Tang, G.; Mayes, M. A.; Parker, J. C.; Jardine, P. M. CXTFIT/Excel−A modular adaptable approach for parameter estimation and uncertainty/sensitivity analysis. *Comput. Geosci.* **2010**, *36*, 1200−1209.

(25) MacIntyre, W. G.; Stauffer, T. B.; Antworth, C. P. Comparison of sorption coefficients determined by batch, column, and box methods on a low organic carbon aquifer material. *Ground Water* **1991**, *29*, 908−913.

(26) Sharma, M. M; Kuo, J. F.; Yen, T. F. Further investigation of the surface charge and properties of oxide surfaces in oil-bearing sands and sandstones. *J. Colloid Interface Sci.* **1987**, *115*, 9−16.

(27) Baker, S.; Green, A.; Williams, S. J. The removal of technetium(VII) from alkaline solution by NRVB, PFA/OPC and

BFS/OPC. *Serco Assurance Report SA/ENV-0606*; Serco: Oxfordshire, 2004.
(28) Hunter, F.; Jackson, C. P. Formal structured data elicitation of technetium solubilities and sorption distribution coefficients in the near field. *Serco Assurance Report SA/ENV-0995*; Serco: Oxfordshire, 2010.
(29) *Geological Disposal: Generic Environmental Safety case main report*, NDA/RWMD/021; Nuclear Decommissioning Authority: Oxcon, UK, December 2010.